

# PDE $\delta$ inhibition impedes the proliferation and survival of human colorectal cancer cell lines harboring oncogenic KRAs

Christian H. Klein<sup>1</sup>, Dina C. Truxius<sup>1</sup>, Holger A. Vogel<sup>1</sup>, Jana Harizanova<sup>1,2</sup>, Sandip Murarka<sup>3</sup>, Pablo Martín-Gago<sup>3</sup> and Philippe I.H. Bastiaens<sup>1,2</sup>

<sup>1</sup>Department of Systemic Cell Biology, Max Planck Institute for Molecular Physiology, Dortmund, Germany

<sup>2</sup>Faculty of Chemistry and Chemical Biology, TU Dortmund, Dortmund, Germany

<sup>3</sup>Department of Chemical Biology, Max Planck Institute for Molecular Physiology, Dortmund, Germany

Ras proteins, most notably KRAs, are prevalent oncogenes in human cancer. Plasma membrane localization and thereby signaling of KRAs is regulated by the prenyl-binding protein PDE $\delta$ . Recently, we have reported the specific anti-proliferative effects of PDE $\delta$  inhibition in KRAs-dependent human pancreatic ductal adenocarcinoma cell lines. Here, we investigated the proliferative dependence on the solubilizing activity of PDE $\delta$  of human colorectal cancer (CRC) cell lines with or without oncogenic KRAs mutations. Our results show that genetic and pharmacologic interference with PDE $\delta$  specifically inhibits proliferation and survival of CRC cell lines harboring oncogenic KRAs mutations whereas isogenic cell lines in which the KRAs oncogene has been removed, or cell lines with oncogenic BRAf mutations or EGFR overexpression are not dependent on PDE $\delta$ . Pharmacological PDE $\delta$  inhibition is therefore a possible new avenue to target oncogenic KRAs bearing CRC.

## Introduction

Ras proteins, most prevalent isoform KRAs4B,<sup>1</sup> are mutated in around 30% of all human cancers<sup>2</sup> and especially frequent in pancreatic, colorectal and lung tumors.<sup>3</sup> Oncogenic mutations retain Ras in a constitutively active conformation,<sup>4</sup> causing sustained activation of downstream signaling cascades leading

**Key words:** KRAs, colorectal cancer, PDE $\delta$ , proliferation

**Abbreviations:** 7-Aminoactinomycin D: 7-AAD; CRC: colorectal cancer; GDI: guanine nucleotide dissociation inhibitor; hPDACs: human pancreatic ductal adenocarcinoma cells; PM: plasma membrane; RE: recycling endosome; RTCA: real-time cell analysis; short hairpin RNA: shRNA

Additional Supporting Information may be found in the online version of this article.

**Conflict of interest:** C.H.K., S.M., P.M.G. and P.I.H.B. are co-inventors on an MPG patent application for Deltasonamide 2. Apart from that, the authors declare no competing financial interest.

**Grant sponsor:** Deutsche Krebshilfe; **Grant numbers:** 110995;

**Grant sponsor:** H2020 European Research Council; **Grant numbers:** 322637

**DOI:** 10.1002/ijc.31859

This is an open access article under the terms of the Creative Commons Attribution-NonCommercial License, which permits use, distribution and reproduction in any medium, provided the original work is properly cited and is not used for commercial purposes.

**History:** Received 27 Jul 2018; Accepted 3 Sep 2018; Online 8 Sep 2018

**Correspondence to:** Philippe I.H. Bastiaens, Department of Systemic Cell Biology, Max Planck Institute for Molecular Physiology, Dortmund, Germany, E-mail: philippe.bastiaens@mpi-dortmund.mpg.de; Tel.: +49(231)-1332200; Fax: +49 (231)-1332299

to increased proliferation and survival.<sup>5</sup> Signal transduction from active KRAs is dependent on its plasma membrane (PM) localization.<sup>6</sup> Despite a polybasic stretch and a farnesyl motif at the C-terminus of KRAs conferring association to the negatively charged inner leaflet of the PM, this localization is compromised by endocytosis and entropy-driven re-equilibration to all endomembranes. The guanine nucleotide dissociation inhibitor (GDI-) like solubilization factor—PDE $\delta$ —counters this re-equilibration by binding the farnesyl-tail of KRAs, thereby effectively increasing diffusion in the cytosol. KRAs is then released in the perinuclear area by activity of the small GTPase Arl2<sup>7,8</sup> and electrostatically trapped and enriched on the recycling endosome (RE). This concentrated KRAs on the RE is transported back to the PM *via* vesicular transport to maintain its enrichment there.<sup>8</sup> Interference with the solubilizing PDE $\delta$  functionality stalls this spatial cycle that maintains KRAs concentration on the PM,<sup>8</sup> thereby impairing KRAs signaling.<sup>8,9</sup>

These findings led to the development of various small-molecule inhibitors of PDE $\delta$  based on different chemical scaffolds (Deltarasin, Deltazinone 1, Deltasonamide 1 and 2) that all competitively interact with the farnesyl-binding pocket.<sup>10–12</sup> In previous studies, we investigated the applicability of these inhibitors on human pancreatic cancer cell lines since the majority (90%) of pancreatic tumors harbor oncogenic KRAs mutations.<sup>3,13</sup> All three inhibitor classes reduced cell proliferation of KRAs-dependent human pancreatic ductal adenocarcinoma cells (hPDACs), whereas KRAs-independent or wild type KRAs harboring hPDACs were less affected.<sup>10–12</sup>

Here, we expand the applicability of pharmacological PDE $\delta$  interference to colorectal cancer (CRC), another tumor

**What's new?**

Oncogenic KRas mutations are present in about 45% of colorectal cancers (CRCs), where they are associated with poor prognosis. While KRas is an appealing therapeutic target, it has repeatedly eluded small-molecule inhibitors. Here, the authors chose instead to target PDE $\delta$ , a prenyl-binding protein that regulates the plasma membrane localization of KRas. In experiments in human colorectal cancer cells, PDE $\delta$  inhibition limited proliferation and survival in cells harboring KRas mutations, with no effect on wild-type KRas cells, providing a new therapeutic opportunity for CRC harbouring oncogenic KRas. In addition, PDE $\delta$  protein expression was correlated with oncogenic KRas activity within the CRC cell panel, suggesting that PDE $\delta$  protein-level determination may be of prognostic relevance for CRC patients.

class with prevalent (45%) oncogenic KRas mutations.<sup>3</sup> To date, targeted therapy with monoclonal antibodies against EGFR, such as Cetuximab, is a major alternative to systemic cytotoxic chemotherapy in CRC.<sup>14</sup> However, therapy based on EGFR inhibition fails if oncogenic KRas<sup>15,16</sup> or BRAF<sup>16,17</sup> are expressed in CRC. To assess if PDE $\delta$  inhibition could be a possible new avenue to affect oncogenic KRas bearing CRC, we studied the dependence of CRC cell proliferation and survival on PDE $\delta$  activity. For this, we compared the effects of doxycycline-induced shRNA mediated down regulation of PDE $\delta$  to the effects of pharmacological interference with PDE $\delta$  activity in a panel of human CRC cell lines harboring distinct oncogenic mutations. We find a high correlation between the effects of pharmacological inhibition and shRNA-mediated PDE $\delta$  knock down on CRC proliferation and survival, where oncogenic KRas bearing CRC cells are highly compromised in cell proliferation and survival, whereas CRC cell lines in which the KRas oncogene was removed, or that harbor other oncogenic mutations, are hardly or not affected by PDE $\delta$  interference. Our findings suggest that PDE $\delta$  could be a valid therapeutic target for oncogenic KRas-driven colorectal cancer.

**Materials and Methods****Cell culture**

HCT-116 (ATCC American Type Culture Collection, Manassas, VA), Hke3 (kind gift from Dr. Owen Sansom), Hkh2 (kind gift from Prof. Dr. Walter Kolch), DiFi (kind gift from Dr. Clara Montagut) and SW480 (ATCC) cell lines were maintained in DMEM (Dulbecco's-modified Eagle medium, Sigma-Aldrich Biochemie GmbH, Taufkirchen, Germany) supplemented with 10% FCS (fetal calf serum; Pan-Biotech GmbH, Aidenbach, Germany), 2 mM L-glutamine (Sigma-Aldrich Biochemie GmbH) and 1% NEAA (nonessential amino acids) (Sigma-Aldrich Biochemie GmbH), at 37 °C and 5% CO<sub>2</sub> in a humidified incubator.

HT29 cells (ATCC) were maintained in Ham's medium (Sigma-Aldrich Biochemie GmbH), supplemented with 10% FCS and 1 mM L-glutamine (Sigma-Aldrich Biochemie GmbH), at 37 °C and 5% CO<sub>2</sub> in a humidified incubator.

Cell line identity was validated by STR-profiling (DSMZ, Braunschweig, Germany) and all cell lines were routinely tested for mycoplasma.

**Virus production and generation of stable cell lines**

Lentiviruses were produced and harvested as described previously, utilizing the most effective shRNA sequence against PDE6D (pLKO-PDE6D-572, see below) from a previous screen.<sup>10</sup> Viral supernatant, containing 10  $\mu$ g/mL polybrene, was immediately used to infect target cells in 6-well plates at 50% confluence. After 24 h, lentivirus-containing supernatant was removed and fresh medium supplied, containing the appropriate amount of puromycin for selection. Puromycin tolerance was tested for all target cell lines prior to shRNA transduction.

*pLKO-shRNA-PDE6D-572:*

5'-CCGGGCACATCCAGAGTGAGACTTTCTCGAGAAA  
GTCTCACTCTGGATGTGCTTTTTT-3'.

**Design of a mCherry-PDE $\delta$  rescue construct and stable expression in HCT-116 cell line**

Eight silent point mutations were introduced into the targeting region of the PDE $\delta$  shRNA of a previously published mCherry-PDE $\delta$  construct<sup>9</sup> using Q5<sup>®</sup> Site-Directed Mutagenesis Kit (New England BioLabs, NEB, Frankfurt, Germany) according to the manufacturer's protocol. After sequence validation, the mutated mCherry-PDE $\delta$  construct was cloned into a PiggyBac vector (System Bioscience, Palo Alto, CA) utilizing the restriction enzymes SpeI and NotI (NEB). Afterwards, HCT-116 cells were co-transfected with the above described construct and a PiggyBac transposase (System Bioscience, ratio 1:1) to enable genome integration. Stable transfected cells were selected by fluorescence activated cell sorting (FACS) based on mCherry fluorescence one week after transfection.

**Western blot analysis**

For PDE $\delta$  protein level analysis, whole cell lysates (WCL) were prepared after 72 h of doxycycline (200 ng/mL) induction as described previously.<sup>11</sup> For enrichment of Ras-GTP, 3xRaf-RBD pull down was executed. Recombinant GST-3xRafRBD<sup>9</sup> was expressed in *E. coli* BL21DE3 by induction with 0.1 mM IPTG for 5 h after the culture reached an OD<sub>600</sub> of 0.8. Afterwards, bacteria were harvested and lysed with bacterial lysis buffer (50 mM Tris-HCl, pH 7.5, 400 mM NaCl, 1 mM DTT, 1% Triton X-100, 1 mM EDTA, supplemented with Complete Mini EDTA-free protease inhibitor (Sigma-Aldrich Biochemie GmbH) and bacterial lysates were stored at -20 °C. For the pull down, 700  $\mu$ g crude bacterial lysate

was incubated with magnetic GSH sepharose 4B beads for 2 h at 4 °C on a rotating wheel and afterwards beads were re-equilibrated in cell lysis buffer (50 mM Tris-HCl pH 7.5, 200 mM NaCl, 10% Glycerol, 2.5 mM MgCl<sub>2</sub>, 1% Triton X-100, supplemented with Complete Mini EDTA-free protease inhibitor). Whole cell lysates were prepared after overnight starvation in cell lysis buffer. 25 µg of WCL were used as “input control” to determine panRas, PDE6D and Cyclophilin B level, whereas 400 µg of WCL was subjected to GST-3xRaf-RBD, bound onto GSH sepharose 4B (GE) beads, pull down. After incubation for 30 min at 4 °C on a rotating wheel, beads were washed three times with cell lysis buffer. Then, bound Ras-GTP was eluted with SDS sample buffer for 10 min at 95 °C. Afterwards, SDS-polyacrylamide gel electrophoresis was carried out. Gels were blotted onto PVDF membrane (Immobilon, Millipore) and blocked for 1 h at room temperature with blocking buffer (LI-COR, Lincoln, NE). For EGF-induced phospho-Erk response analysis in SW480 and HT29, cells were starved for 16 h prior to incubation for 90 min with 5 or 10 µM of Deltarasin/Deltasonamide 2. Afterwards, cells were stimulated with 100 ng/mL EGF for 5 min and subsequently washed with ice-cold PBS and lysed in 100 µL ice-cold lysis buffer containing protease inhibitors (Roche) and phosphatase inhibitor I and II (Sigma-Aldrich Biochemie GmbH). Lysates were further processed as described above. The following antibodies were used for western blotting in the stated dilution: anti-PDE6D (Santa Cruz: sc-50260, 1:200), anti-Cyclophilin-B (Abcam: Ab16045, 1:3,000), anti-panRas (Calbiochem: OP40, 1:1,000), anti-mCherry (Abcam: Ab167453, 1:1,000), anti-α-Tubulin (Sigma: T6074, 1:3,000), anti-Erk1/2 (Abcam: Ab36991; 1:1,000), Phospho-p44/42 (Erk1/2) (Thr202/Tyr204) (Cell Signaling Technology: #4370, 1:1,000) and matching secondary infrared antibodies IRDye 680 donkey anti rabbit IgG, IRDye 800 donkey anti mouse/goat IgG, (LI-COR, 1:10,000). Blots were scanned on a LI-COR Odyssey imaging system. Western blots were quantified using the Gel profiler plugin of ImageJ. Uncropped blots are shown in Supporting Information Figures 1, 2 and 7.

### RT-qPCR

To determine PDE6D and KRas mRNA level in CRC cell lines, RNA was isolated using a RNA extraction kit (Zymo Research, Irvine, CA) according to the manufacturer's protocol. 2 µg isolated RNA of each cell lysate were used to perform RT-PCR according to the manufacturer's protocol (High Capacity cDNA Reverse Transcription Kit; Thermo Fisher Scientific), yielding 2 µg cDNA. For quantitative PCR, commercial available TaqMan<sup>®</sup>-assays (Thermo Fisher Scientific) for PDE6D (Hs01062025\_m1), KRas (Hs00364282\_m1) and GAPDH (Hs02758991\_g1) were utilized according to the manufacturer's protocol. ΔCT-values were calculated by subtracting the CT values of the housekeeping gene GAPDH from either KRas CT or PDE6D CT values.

### *In silico* analysis of PDE6D and KRas mRNA expression in CRC patient data

For the *in silico* analysis of available patient data, a dataset containing KRas and PDE6D mRNA expression data of 195 CRC patients, including mutation status of the KRas gene, was downloaded from The Cancer Genome Atlas (TCGA).<sup>18</sup> Patient data was separated into wild type KRas (*n* = 108) and mutant KRas (*n* = 87) cases and compared with regard to differences in their mRNA expression levels of KRas and PDE6D. For correlation analysis KRas mRNA expression levels were plotted *vs.* corresponding PDE6D mRNA expression levels and Pearson's correlation coefficient was determined.

### Clonogenic assays

Sparsely seeded cells ( $1 \times 10^3$ – $2 \times 10^3$  per well) were maintained in a 6-well plate in the presence or absence of doxycycline (200 ng/ml). Doxycycline was applied 24 h after seeding. After ten days, cells were fixed and stained with 0.05% (v/v) crystal violet (Sigma-Aldrich Biochemie GmbH) to visualize individual colonies. The quantification was performed using the analyze particle plug-in of ImageJ to extract total cell number and average colony size after utilizing a cell profiler pipeline to separate overlapping colonies.

### Real-time cell analyzer

Real-time cell analyzer (RTCA) measurements were performed using 16-well E-plates on a Dual Plate xCELLigence instrument (Roche Applied Science, Penzberg, Germany) in a humidified incubator at 37 °C with 5% CO<sub>2</sub>. The system measures the impedance-based cell index (CI), a dimensionless parameter which evaluates the ionic environment at the electrode/solution interface and integrates this information on the cell number.<sup>19</sup> Continuous impedance measurements were monitored every 15 min for up to 300 h. Blank measurements were performed with growth medium. Depending on the cell line,  $1 \times 10^4$ – $2 \times 10^4$  cells were plated in each well of the 16-well plates for short-term measurements and  $0.75$ – $2 \times 10^3$  cells/well for long-term measurements. After seeding, cells were allowed to reach steady growth for 24 h before small-molecule inhibitor administration, whereas in case of cells stably expressing the inducible shRNA against PDE6 or non-targeting shRNA, doxycycline was directly applied to the wells. In case of dose-dependent inhibitor measurements, the amount of DMSO was kept constant between the individual conditions and did not exceed 0.24%. Cell indices were normalized to the time point of drug administration. For shRNA experiments no normalization was applied.

### Apoptosis assay

Apoptosis assays were performed on a LSR II flow cytometer (BD Bioscience, Heidelberg, Germany). Cells were seeded in 6-well plates at  $2 \times 10^5$  cells per well and treated with different concentrations of small-molecule inhibitors (Deltarasin or

Deltasonamide 2) for 24 h. DMSO was used as a vehicle control. Subsequently, the supernatant was collected in FACS vials and the cells were washed with 1 mL PBS. Afterwards, cells were detached with 0.5 mL Accutase™ (EMD Millipore Corporation). The detached cells were re-suspended in 1 mL PBS and transferred to the respective FACS vials and centrifuged at 200 g for 5 min. The supernatant was discarded and the cells were washed twice with PBS. Cell pellets were re-suspended in 100  $\mu$ L PBS containing 5  $\mu$ L of 7-AAD (BD Bioscience). Samples were vortexed and incubated in the dark at RT for 15 min. Afterwards, 200  $\mu$ L PBS was added and the samples transferred to FACS vials through filter lids. The fluorescence of single cells in flow through was measured within one hour after transfer through a 695/40 emission filter using the 488 nm argon laser line for excitation. Measurements were acquired and gated with the BD FACSDiva™ software.

### Small-molecule inhibitors

Deltarasin (Lot. No. 1) was purchased from Chemietek, Indianapolis, IN. Deltasonamide 2 was synthesized in-house as described previously.<sup>12</sup> For RTCA, Deltarasin was used in a concentration range of 1–13  $\mu$ M and Deltasonamide 2 in a concentration range of 0.375–12  $\mu$ M. For apoptosis assays, inhibitors were used in a concentration range of 1–7  $\mu$ M (Deltarasin) and 1–5  $\mu$ M (Deltasonamide 2), respectively.

### Results and Discussion

We studied the effects of genetic and pharmacological PDE $\delta$  interference in a cell panel containing six human CRC cell lines lacking or bearing distinct oncogenic mutations (Table 1). While the SW480 cell line is homozygote for oncogenic KRas,<sup>20</sup> HCT-116 cells contain one mutant and one wild type KRas allele.<sup>21</sup> With the goal to create isogenic cell lines to HCT-116 that do not harbor oncogenic KRas, the Hke3 and Hkh2 cell lines were derived from HCT-116 by exchanging the mutant KRas allele with a nontranscribed KRas mutant (G12C) allele using homologous recombination.<sup>21</sup> However, the recombination was only successful in Hkh2, while Hke3 cells still contain an allele encoding oncogenic KRas that is expressed at lower levels (dosage effect mutant).<sup>22</sup> In addition, we studied two CRC cell lines expressing wild type KRas that have other oncogenic mutations. The HT29

cell line bears an oncogenic BRAf mutation (V600E),<sup>17</sup> an effector of Ras,<sup>23</sup> whereas DiFi cells harbor an amplification of the EGFR gene accompanied with increased level of EGFR protein expression<sup>24,25</sup> and are one of the few available cell models that are sensitive to anti-EGFR mAb treatment.<sup>26</sup>

To study effects of PDE $\delta$  knock down on proliferation and viability, CRC cells were transduced with a lentivirus encoding a previously reported doxycycline-inducible short hairpin RNA (shRNA) sequence against PDE $\delta$  or a nontargeting shRNA (scrambled, scr) control that is stably incorporated into their genome.<sup>10,11</sup> shRNA expression was induced by doxycycline over several days and PDE $\delta$  protein levels were determined by western blot analysis at different time points in Hke3 cells. PDE $\delta$  levels decreased over time after doxycycline induction and a good knock down efficiency of >80% was reached after 72 h (Supporting Information Fig. 1 A), which is consistent with the low protein turnover of PDE $\delta$ .<sup>9</sup> To now compare the amount of PDE $\delta$  expression levels of the different cell lines as well as to evaluate the knock down efficiency, western blot analysis of PDE $\delta$  protein levels was performed with/without doxycycline induction for 72 h (Fig. 1a). All transduced stable shRNA-PDE $\delta$  cell lines showed a clear reduction in PDE $\delta$  protein levels upon doxycycline induction, in contrast to doxycycline induction of scrambled shRNA (Supporting Information Fig. 1 D). Comparison of PDE $\delta$  expression levels in the noninduced CRC cell lines revealed that SW480 cells (homozygote for KRasG12V) exhibited the highest PDE $\delta$  level, whereas the KRas wild type expressing HT29 cell line contained the lowest amount of PDE $\delta$  protein. Since PDE $\delta$  is necessary to maintain the PM localization of KRas and thereby its signaling activity,<sup>8,9</sup> we next investigated if there was a correlation between PDE $\delta$  expression and KRas activity among the different CRC cell lines. For this, we quantified the expression levels of PDE $\delta$  and Ras within the parental cell lines by western blot analysis (Fig. 1b). The amount of GTP-loaded Ras was also quantified by specific precipitation of Ras-GTP from whole cell lysates using 3xRBD (three repeats of Ras binding domain of cRaf<sup>9</sup>) from cells that were serum-starved 24 h prior to cell lysis. A strong correlation between PDE $\delta$  levels and total Ras expression (Pearson's correlation coefficient of  $r^2 = 0.974$ ) as well as Ras activity ( $r^2 = 0.949$ ) became apparent, suggesting a dependence of oncogenic Ras activity on PDE $\delta$  expression levels. We next investigated if this Ras-PDE $\delta$  protein expression correlation is mirrored on the mRNA level in cancer cells of CRC patients and could provide a potential prognostic indicator. For this, mRNA expression data for PDE6D and KRas from 195 CRC patients was extracted from the Cancer Genome Atlas (TCGA)<sup>18</sup> The patient data was divided into KRas wild type (red,  $n = 108$ ) and mutant KRas (blue,  $n = 87$ ) cases. The KRas mRNA expression levels were significantly increased in CRC patients with KRas mutation, while the PDE6D mRNA expression was comparable in both cases (Supporting Information Fig. 3A). Correlation analysis of PDE6D and KRas

**Table 1.** Overview of colorectal cancer cell lines used in our study including KRas mutation status as well as other relevant oncogenic mutations

Cell line	KRas status	Other onc. Mutations
SW480	G12V//G12V	–
HCT-116	G13D//wt	–
Hke3	G13D//wt	–
Hkh2	–//wt	–
HT29	wt//wt	BRaf (V600E)
DiFi	wt//wt	EGFR overexpression



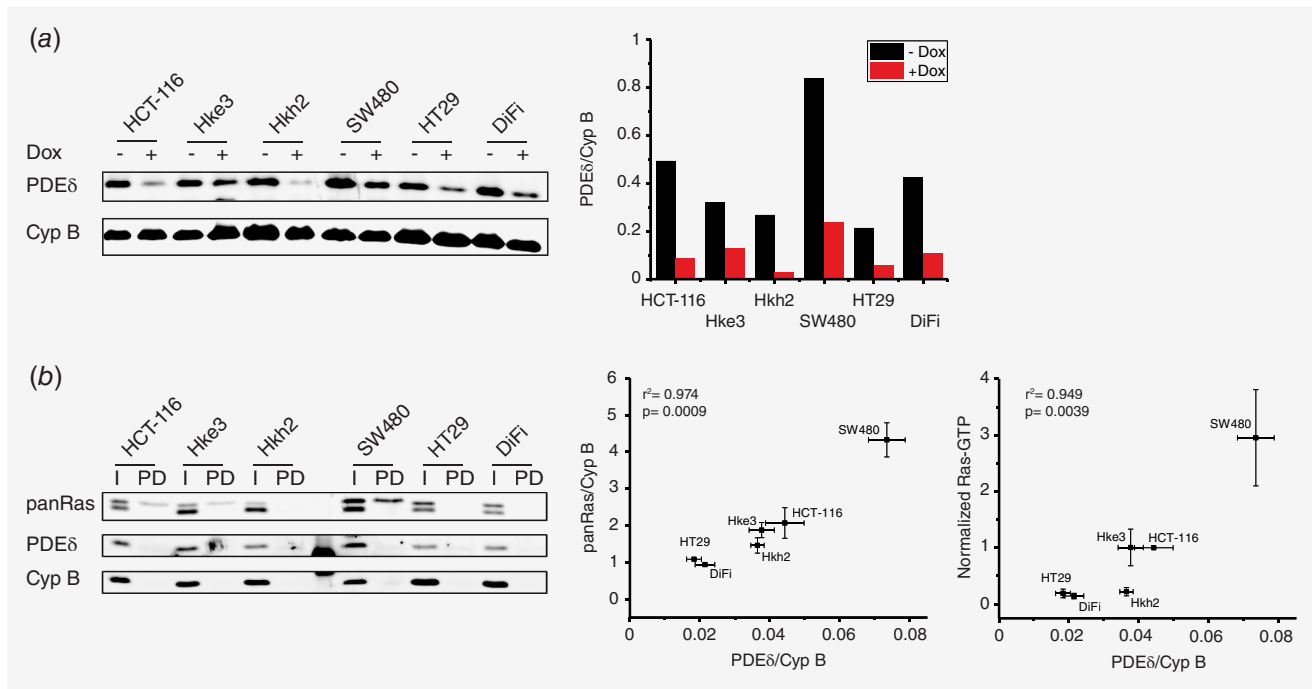


**Figure 1.** PDE $\delta$  and Ras levels in colorectal cancer cell lines. (a) Left: PDE $\delta$  protein level of distinct colorectal cancer cell lines in absence or presence of PDE $\delta$  shRNA induced by doxycycline after 72 h determined by western blot analysis. Cyclophilin B was used as loading control. Right bar graph: quantification of endogenous PDE $\delta$  levels of each cell line with (red) and without (black) doxycycline induction. (b) Left: PDE $\delta$  and panRas protein level (I) and Ras-GTP level (PD) of distinct CRC cell lines determined by western blot analysis. Cells were serum-starved 24 h before lysis and active Ras was enriched by 3xRaf-RBD pull-down. Middle and right: Correlation plots of PDE $\delta$  and panRas expression  $\pm$  s.e.m of four biological replicates as well as PDE $\delta$  and active Ras levels  $\pm$  s.e.m of four biological replicates (normalized to HCT-116 data). Pearson's correlation analysis shows a high correlation of 0.974 and 0.949 between the respective expression levels. [Color figure can be viewed at [wileyonlinelibrary.com](http://wileyonlinelibrary.com)]

mRNA expression showed only a weak correlation in the CRC patient dataset ( $r^2 = 0.262$ ) (Supporting Information Fig. 3B). Since the TCGA dataset only contains information on mRNA and not protein expression, we utilized RT-qPCR to determine if PDE6D and KRas mRNA expression levels within our CRC cell panel correlates with protein expression. Consistent with the CRC patient data, mRNA expression levels of PDE6D and KRas showed no correlation within the CRC cell panel ( $r^2 = -0.161$ ) (Supporting Information Fig. 3C). However, neither PDE6D nor KRas mRNA levels were correlated to their respective protein expression level (Supporting Information Fig. 3D). This indicates that mRNA expression of PDE $\delta$  has no prognostic relevance for CRC. However, the clear correlation we found between oncogenic KRas activity and PDE $\delta$  expression on the protein level would indicate that PDE $\delta$  protein level determination could be of prognostic value as an indicator of the level of oncogenic Ras signaling activity in CRC. The correlation between KRas signaling activity and PDE $\delta$  expression levels indicates that KRas signaling induces a homeostatic PDE $\delta$  expression mechanism to maintain its own activity at the PM.

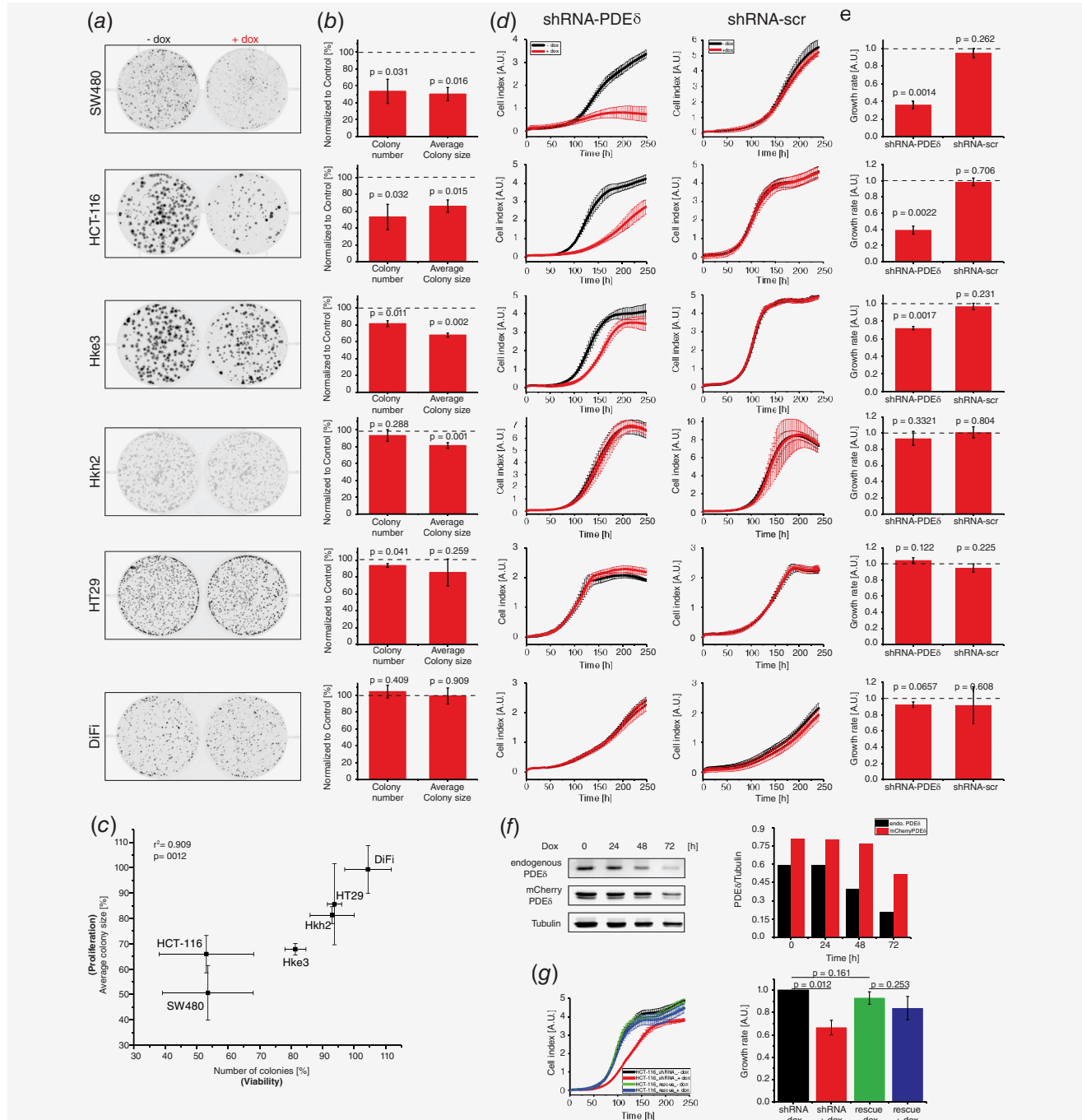
We next performed clonogenic assays<sup>27</sup> to study the effect of doxycycline induced PDE $\delta$  knock down on proliferation and viability of the different CRC cell lines (Fig. 2a). For this, CRC cells stably transduced with doxycycline-inducible

shRNA against PDE $\delta$  were grown in the presence of doxycycline and the colony number and size was compared to that of untreated control after a growth period of ten days. Here, the number of colonies that remain after PDE $\delta$  knock down is a measure of cell viability, whereas the colony size is a measure of cell proliferation. Quantification of these two parameters (Fig. 2b) showed significant growth-inhibition and viability reduction as a result of PDE $\delta$  knock down only in the oncogenic KRas bearing SW480, HCT-116 and Hke3 cell lines, but not in the HT29 cell line (oncogenic BRAFV600E) and DiFi cells with EGFR overexpression, while the isogenic oncogenic KRas-lacking Hkh2 cell line showed only a minimal decrease in cell proliferation. A clear correlation between oncogenic KRas expression and viability as well as proliferation could be observed upon doxycycline induced PDE $\delta$  knock down in the CRC cells (Fig. 2c, Pearson's correlation coefficient of  $r^2 = 0.909$ ). A clear separation of CRC cells with and without KRas mutation became also apparent. SW480 cells, in which both KRas alleles are mutated, exhibited the strongest reduction in proliferation and cell viability. Both HCT-116 and Hke3 cells (heterozygote KRasG13D) showed a comparable reduction in cell proliferation upon PDE $\delta$  knock down, whereas the viability of the low oncogenic KRas-expressing Hke3 was substantially less affected. In contrast, the wild type KRas bearing CRC cells

(HT29, Hkh2) were hardly affected in their viability and proliferation and DiFi cells were not affected at all.

The clonogenic assays were complemented with real-time cell analysis (RTCA), where changes in the coverage of a surface by cells is measured by impedance (Fig. 2d).<sup>19</sup> Consistent with the clonogenic assays, PDE $\delta$  knock down resulted in a strongly reduced proliferation of CRC cell lines harboring oncogenic KRas, while the induction of nontargeting (scrambled) shRNA had no effect on cell proliferation. Growth rates

of KRas wild type cell lines Hkh2, HT29 and DiFi were again comparable to the respective controls (Fig. 2e). The CRC cells with heterozygote oncogenic KRas mutation (HCT-116 and Hke3) both exhibited reduced cell proliferation upon doxycycline induction. However, whereas Hke3 only exhibited a delay in cell proliferation after doxycycline administration, the rate of proliferation was affected in HCT-116, resulting in a substantially reduced cell number. In contrast, the growth rate of homozygote oncogenic KRas mutation bearing SW480 cells



completely stagnated after doxycycline administration and cell death became apparent after 175 h from the negative growth rate (decrease in cell index). To validate that the observed effects on cell proliferation were caused by PDE $\delta$  knock down, we engineered the HCT-116 cell line harboring the doxycycline-inducible shRNA against PDE $\delta$  to stably express a mCherry-tagged PDE $\delta$  rescue construct with eight silent mutations in the shRNA-PDE $\delta$  binding sequence. This construct largely resists shRNA induced degradation. shRNA expression was induced by doxycycline over several days and endogenous PDE $\delta$  as well as rescue mCherry-PDE $\delta$  protein level were determined by western blot analysis at different time points. Endogenous PDE $\delta$  protein levels decreased to ~25% after doxycycline induction, whereas the expression of the “rescue” mCherry-PDE $\delta$  protein was affected to a much lesser extent (~63%, Fig. 2f). Complementary to this, the growth rate of rescue mCherry-PDE $\delta$  expressing HCT-116 cells was unaffected by doxycycline induced shRNA-PDE $\delta$  expression in contrast to HCT-116 cells (Fig. 2g). This further confirms that PDE $\delta$  expression is necessary for oncogenic KRas signaling in CRC.

We next compared the effects of two small-molecule PDE $\delta$  inhibitors with different chemotypes, Deltarasin<sup>10</sup> and Deltasonamide 2<sup>12</sup> (Fig. 3a, f), on growth rate and cell viability within the CRC cell panel. Both inhibitors competitively bind to the hydrophobic binding pocket of PDE $\delta$  as mediated by hydrogen bonds (H-bonds). However, while Deltarasin engages only in 3 H-bonds exhibiting a corresponding moderate affinity ( $K_D = 38 \pm 16$  nM),<sup>10</sup> Deltasonamide 2 engages in 7 H-bonds and exhibits a high affinity ( $K_D = 385 \pm 52$  pM).<sup>12</sup> To determine the effects of the dose of inhibitors on proliferation, we performed RTCA measurements for cell growth (Fig. 3b, g; Supporting Information Fig. 4) and flow cytometry-based 7-AAD (7-Aminoactinomycin D) single cell fluorescence assays that report on cell death<sup>28</sup> (Fig. 3c, h; Supporting Information Figs. 5, 6). We related the effects of the inhibitors on proliferation and cell viability by determining

EC<sub>50</sub> values by sigmoidal curve fitting of the calculated growth rates against inhibitor dose and plotted these against the difference in cell viability at highest inhibitor dose in comparison to the DMSO control ( $\Delta$  cell viability). In these inhibitor correlation plots (Fig. 3d, i), SW480 exhibited the lowest EC<sub>50</sub> (Deltarasin:  $2.86 \pm 0.31$   $\mu$ M, Deltasonamide2:  $1.24 \pm 0.06$   $\mu$ M) as well as highly compromised viability. The three isogenic cell lines (HCT-116, Hke3, Hkh2) showed comparable EC<sub>50</sub> values, while cell viability of oncogenic KRas-lacking Hkh2 was less affected compared to HCT-116 and Hke3. The DiFi and HT29 cells that lack oncogenic KRas were clearly separated from oncogenic KRas harboring cell lines, where DiFi exhibited the highest EC<sub>50</sub> (Deltarasin:  $8.92 \pm 0.7$   $\mu$ M, Deltasonamide2:  $4.02 \pm 1$   $\mu$ M) and HT29 viability was not affected by inhibitor administration. As expected, the high affinity inhibitor Deltasonamide 2 showed a shift to lower EC<sub>50</sub> values for all CRC cell lines. Strikingly, the correlation plots of both Deltarasin (Fig. 3d) and Deltasonamide 2 (Fig. 3i) showed a similar alignment of cell lines with respect to their KRas mutation status and this alignment was reminiscent to that of PDE $\delta$  knock down (Fig. 2c). This further strengthens the argument<sup>10,12</sup> that the effect of the inhibitors on proliferation is due to specific targeting of PDE $\delta$ . To further compare dose–response profiles between Deltarasin and Deltasonamide 2, we plotted viability (7-AAD staining) vs. growth rate (RTCA) in dependence of the respective inhibitor dose and cell line (Fig. 3e, j). This again revealed the similarity in dose–response profiles between SW480, HCT-116 and Hke3 regarding reduced viability and growth for both inhibitors. The wild type KRas cell lines were clearly less affected in both proliferation readouts, with the HCT-116-derived Hkh2 cells being the most responsive to the inhibitory effects on growth rate and viability.

To examine whether the inhibitory effects of the drugs on cell proliferation and viability are caused by down regulation of oncogenic KRas signaling, we examined the phosphorylation response of the extracellular signal regulated kinase (Erk)<sup>29</sup> to

**Figure 2.** PDE $\delta$  knock down suppresses proliferation and survival of colorectal cancer cell lines harboring oncogenic KRas mutations. (a) Representative example out of three independent clonogenic assay experiments for the cell lines indicated. Cells were grown for ten days in the presence (+dox) or absence (–dox) of doxycycline. (b) Quantification of colony number  $\pm$  s.d. and average colony size  $\pm$  s.d. of three independent experiments. Knock down wells were normalized to the respective untreated control (dashed line). Significance was calculated using one sample *t* test. (c) Correlation plot of colony number  $\pm$  s.d. vs. average colony size  $\pm$  s.d. relative to respective control conditions under PDE $\delta$  knock down as determined in (b). Pearson’s correlation analysis shows a correlation of 0.909. (d) Representative RTCA profiles out of three independent experiments for shRNA against PDE $\delta$  or nontargeting (scr) shRNA. Cell indices  $\pm$  s.d. of four replicates were measured in the presence (red) or absence (black) of doxycycline. Doxycycline was added at the beginning of the measurement. (e) Growth rates  $\pm$  s.d. of doxycycline-induced shRNA-PDE $\delta$  or scrambled shRNA expression of three independent experiments. Growth rates were calculated by the area under RTCA curve over 240 h and normalized to the respective untreated condition (dashed line). Significance was calculated using one sample *t* test. (f) Left: endogenous PDE $\delta$  and rescue mCherry-PDE $\delta$  protein level in HCT-116 after increasing periods of doxycycline administration determined by western blot. Tubulin was used as loading control. Right bar graph: quantification of endogenous PDE $\delta$  (black) and mCherry-PDE $\delta$  (red) levels after different administration periods. (g) Left: Representative RTCA profile out of three independent experiments for HCT-116 shRNA PDE $\delta$  (black, red) and HCT-116 shRNA PDE $\delta$  stably expressing a rescue mCherry-PDE $\delta$  construct (blue, green). Cell indices  $\pm$  s.d. of four replicates were measured in the presence (red, blue) or absence (black, green) of doxycycline. Doxycycline was added at the beginning of the measurement. Right: Growth rates  $\pm$  s.d. ( $n = 3$ ) of doxycycline-induced shRNA-PDE $\delta$  in HCT-116 with and without mCherry-PDE $\delta$  rescue construct expression. Growth rates were calculated by the area under RTCA curve over 240 h and normalized to the untreated control (black). Significance was calculated using student’s *t* test.

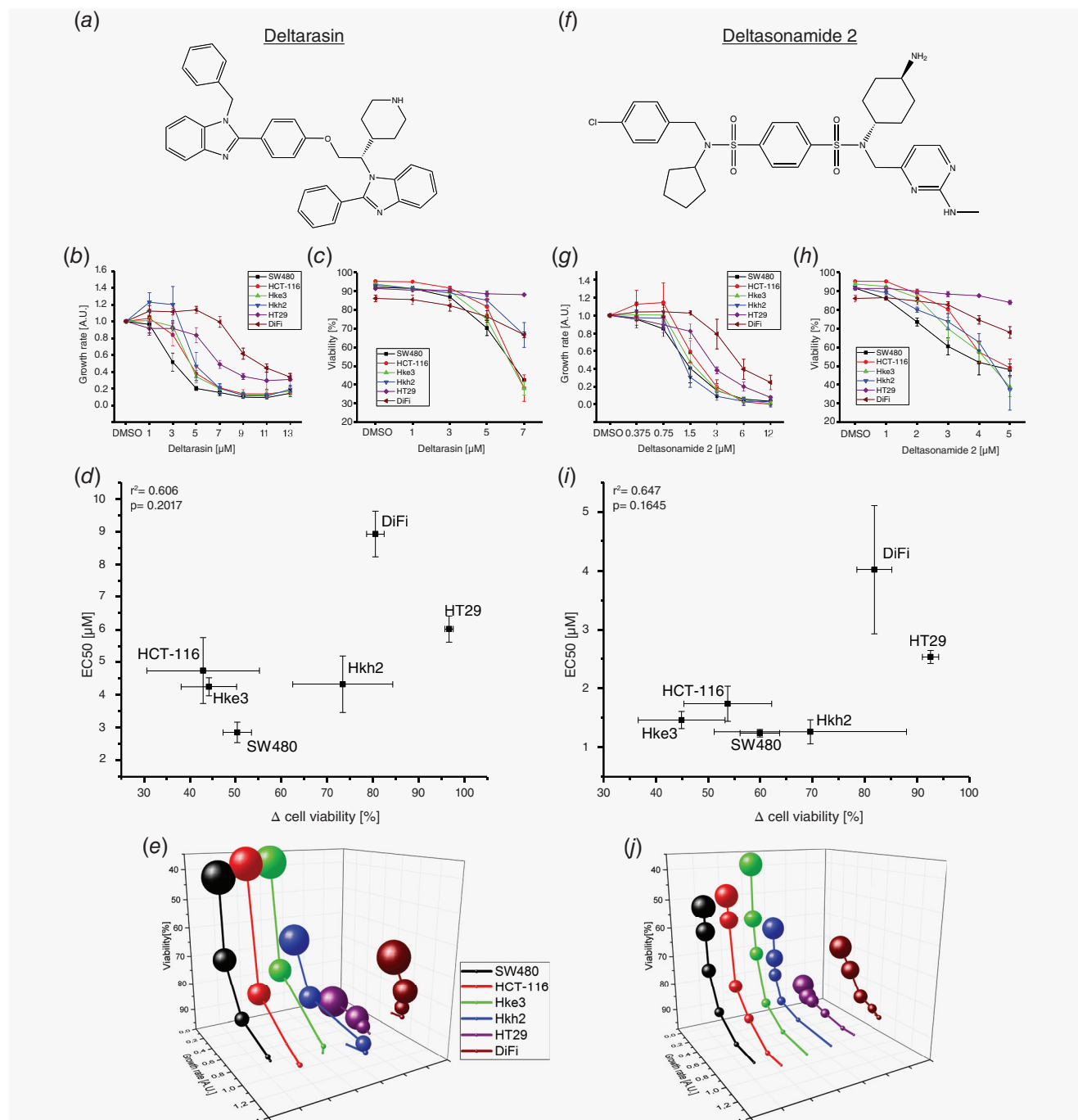


**Figure 3.** Dose-dependent inhibition of proliferation and viability in human colorectal cancer cell lines by PDE $\delta$  inhibitors. (a, f) Chemical structures of the small molecule PDE $\delta$  inhibitors Deltarasin and Deltasonamide 2. (b, g) Growth rate  $\pm$  s.d. in dependence of Deltarasin or Deltasonamide 2 dose. Growth rates were determined by integration of the area below the RTCA curves (Supporting Information Fig. 4) over 60 h after drug administration and normalized to the DMSO control. (c, h) Cell viability  $\pm$  s.d. in dependence of Deltarasin or Deltasonamide 2 dose in CRC cell lines after 24 h of drug administration. Cell death was determined by viability staining using 7-AAD. DMSO was used as vehicle control. (d, i) Correlation of  $\Delta$  Cell viability  $\pm$  s.d. vs. EC<sub>50</sub>  $\pm$  s.d. for Deltarasin (d) and Deltasonamide 2 (i).  $\Delta$  cell viability was calculated between DMSO control and the highest used inhibitor concentration, respectively. EC<sub>50</sub> values were determined by sigmoidal curve fit of the growth rates depicted in b and g. (e, j) Four-dimensional correlation of growth rate and cell viability in dependence of inhibitor dose and CRC cell line for Deltarasin (e) and Deltasonamide 2 (j). The sphere size is proportional to the applied inhibitor concentration.



5 min EGF stimulation in the oncogenic KRas expressing SW480 cells and the KRas wild type expressing HT29 cell line after 90 min Deltarasin or Deltasonamide 2 administration (Supporting Information Fig. 7A). In SW480, both inhibitors reduced Erk phosphorylation with respect to the control, where the superior high affinity inhibitor, Deltasonamide 2, reduced it as much as ~80%. In contrast, the Erk response was not affected in HT29 cells upon treatment with Deltasonamide 2 and increased upon Deltarasin administration. This could represent an antagonistic off-target effect of the lower affinity inhibitor Deltarasin, which is known to also affect other signaling proteins.<sup>11</sup>

Both PDE $\delta$  knock down and small-molecule inhibition were most effective in SW480 cells, which are homozygote for oncogenic KRas.<sup>20</sup> SW480 also exhibited the highest expression levels of Ras and PDE $\delta$ . Together, this implies that proliferation and survival of SW480 are depending on oncogenic KRas (and thereby PDE $\delta$ ) and that these cells have no compensatory mechanism to rescue for PDE $\delta$  loss or inhibition. The isogenic cell lines HCT-116, Hke3 and Hkh2 are a well-suited system to study effects of PDE $\delta$  interference in a presumably isogenic background since they should only differ in their KRas mutation status.<sup>21</sup> Our results (Fig. 1b) however showed that Hke3 cells still possess GTP-loaded Ras under serum-starved conditions and thereby confirmed that they still harbor an oncogenic KRas mutation.<sup>22</sup> In contrast, the oncogenic allele was successfully removed in the Hkh2 cell line, manifested in the low level of detected Ras-GTP (Fig. 1b). Indeed, the parental HCT-116 cell line showed a stronger reduction in cell growth and viability by PDE $\delta$  knock down or inhibitor treatment compared to Hkh2. In contrast, effects on growth rate and cell viability were comparable between HCT-116 and Hke3 after PDE $\delta$  inhibition, whereas cell viability of Hke3 was less affected by PDE $\delta$  knock down. This indicates that the oncogenic KRas expression levels are an important determinant for cell survival but less for proliferation in CRC cells. This would also point at that oncogene addition is related to the expression level of the oncogene.<sup>30</sup>

Strikingly, the proliferation and survival of BRaf(V600E) bearing HT29<sup>17</sup> and EGFR overexpressing DiFi<sup>24,25</sup> was not affected by PDE $\delta$  knockout and were the least sensitive to both tested PDE $\delta$  inhibitors. In the MAP kinase signaling network,<sup>29</sup> BRaf is activated downstream of KRas, making those cells that harbor the BRaf(V600E) mutation independent of KRas signal input and thereby its localization. This is consistent with PDE $\delta$  interference not affecting the

proliferation of these cells. However, DiFi cells feature an up-regulated EGFR expression level<sup>24,25</sup> and EGFR is located upstream of KRas in the MAP kinase signaling network. One would therefore assume that PDE $\delta$  down modulation would affect signal propagation in the MAPK network in these cells, which was not the case. However, DiFi cells also exhibit low levels of Ras protein (Fig. 1b), and it is therefore likely that other signals emanate from overexpressed EGFR, possibly *via* the PI3K-Akt axis, that sustain proliferation and survival. Both DiFi and HT29 cells, expressed the lowest amount of PDE $\delta$  as well as Ras proteins among our tested CRC cell lines, and PDE $\delta$  expression level was correlated to oncogenic Ras activity. This indicates the interdependence of oncogenic Ras activity and the solubilizing activity of PDE $\delta$  that can be exploited to affect oncogenic KRas signaling in cancer cells by inhibition of PDE $\delta$ . Indeed, small molecule inhibition of PDE $\delta$  in these CRC cell lines phenocopied PDE $\delta$  knock down. The latest generation of high affinity PDE $\delta$  inhibitors such as Deltasonamide 2 thereby proved to be the superior inhibitor.<sup>12</sup> The discrepancy between the  $\mu$ M concentration of Deltasonamide 2 that induce a growth inhibitory effect and its  $K_D$  for PDE $\delta$  (~385 pM) is due to its low partitioning in the cytosol. However, our results show that potent inhibitors of the KRas-PDE $\delta$  interaction might impair the growth of CRC driven by oncogenic KRas and may offer new therapeutic angles for colorectal cancers harboring oncogenic KRas mutations that are unresponsive to treatment.<sup>14,15</sup>

### Acknowledgment

This research was supported by the Deutsche Krebshilfe (Grant 110995) and the European Research Council (ERC Grant 322637). The results shown in Supporting Information Figure 3A and B are based upon data generated by the TCGA Research Network: <http://cancergenome.nih.gov/>.

### Author contributions

P.I.H.B. conceived the project. D.C.T. and C.H.K. generated stable inducible shRNA-PDE $\delta$  cell lines. C.H.K. and D.C.T. performed western blot analysis. C.H.K. performed clonogenic assays and J.H. and C.H.K. analyzed the data. C.H.K. and H.A.V. performed real-time cell analysis measurements. C.H.K. performed viability assays, RT-qPCR measurements and *in silico* analysis. S.M. and P.M.G. synthesized Deltasonamide 2. C.H.K. and P.I.H.B. wrote the study.

### References

1. Aguirre AJ, Bardeesy N, Sinha M, et al. Activated Kras and Ink4a/Arf deficiency cooperate to produce metastatic pancreatic ductal adenocarcinoma. *Genes Dev* 2003;17:3112–26.
2. Forbes SA, Bindal N, Bamford S, et al. COSMIC: mining complete cancer genomes in the catalogue of somatic mutations in cancer. *Nucleic Acids Res* 2011;39:D945–50.
3. Cox AD, Fesik SW, Kimmelman AC, et al. Drugging the undruggable RAS: Mission possible? *Nat Rev Drug Discov* 2014;13:828–51.
4. Wittinghofer A. Signal transduction via Ras. *Biol Chem* 1998;379:933–7.
5. Karnoub AE, Weinberg RA. Ras oncogenes: split personalities. *Nat Rev Mol Cell Biol* 2008;9:517–31.
6. Schmick M, Kraemer A, Bastiaens PI. Ras moves to stay in place. *Trends Cell Biol* 2015;25:190–7.
7. Ismail SA, Chen YX, Rusinova A, et al. Arl2-GTP and Arl3-GTP regulate a GDI-like transport system for farnesylated cargo. *Nat Chem Biol* 2011;7:942–9.
8. Schmick M, Vartak N, Papke B, et al. KRas localizes to the plasma membrane by spatial cycles of

- solubilization, trapping and vesicular transport. *Cell* 2014;157:459–71.
9. Chandra A, Grecco HE, Pisupati V, et al. The GDI-like solubilizing factor PDE $\delta$  sustains the spatial organization and signalling of Ras family proteins. *Nat Cell Biol* 2011;14:148–58.
  10. Zimmermann G, Papke B, Ismail S, et al. Small molecule inhibition of the KRAS-PDE $\delta$  interaction impairs oncogenic KRAS signalling. *Nature* 2013;497:638–42.
  11. Papke B, Murarka S, Vogel HA, et al. Identification of pyrazolopyridazinones as PDE $\delta$  inhibitors. *Nat Commun* 2016;7:11360.
  12. Martin-Gago P, Fansa EK, Klein CH, et al. A PDE $\delta$ -KRas inhibitor Chemotype with up to seven H-bonds and Picomolar affinity that prevents efficient inhibitor release by Arl2. *Angew Chem Int Ed Engl* 2017;56:2423–8.
  13. Papke B, Der CJ. Drugging RAS: know the enemy. *Science* 2017;355:1158–63.
  14. Humblet Y. Cetuximab: an IgG(1) monoclonal antibody for the treatment of epidermal growth factor receptor-expressing tumours. *Expert Opin Pharmacother* 2004;5:1621–33.
  15. Misale S, Yaeger R, Hobor S, et al. Emergence of KRAS mutations and acquired resistance to anti-EGFR therapy in colorectal cancer. *Nature* 2012;486:532–6.
  16. Benvenuti S, Sartore-Bianchi A, Di Nicolantonio F, et al. Oncogenic activation of the RAS/RAF signaling pathway impairs the response of metastatic colorectal cancers to anti-epidermal growth factor receptor antibody therapies. *Cancer Res* 2007;67:2643–8.
  17. Di Nicolantonio F, Martini M, Molinari F, et al. Wild-type BRAF is required for response to panitumumab or cetuximab in metastatic colorectal cancer. *J Clin Oncol* 2008;26:5705–12.
  18. Cancer Genome Atlas N. Comprehensive molecular characterization of human colon and rectal cancer. *Nature* 2012;487:330–7.
  19. Abassi YA, Jackson JA, Zhu J, et al. Label-free, real-time monitoring of IgE-mediated mast cell activation on microelectronic cell sensor arrays. *J Immunol Methods* 2004;292:195–205.
  20. Ahmed D, Eide PW, Eilertsen IA, et al. Epigenetic and genetic features of 24 colon cancer cell lines. *Oncogene* 2013;2:e71.
  21. S Shirasawa MF, Yokoyama N, Sasazuki T. Altered growth of human colon cancer cell lines disrupted at activated Ki-ras. *Science* 1993;260:85–8.
  22. FASTER E, Raso C, Kennedy S, et al. A novel RNA sequencing data analysis method for cell line authentication. *PLoS One* 2017;12:e0171435.
  23. Marais R, Light Y, Paterson HF, et al. Ras recruits Raf-1 to the plasma membrane for activation by tyrosine phosphorylation. *EMBO J* 1995;14:3136–45.
  24. Gross ME, Zorbas MA, Danels YJ, et al. Cellular growth response to epidermal growth factor in colon carcinoma cells with an amplified epidermal growth factor receptor derived from a familial adenomatous polyposis patient. *Cancer Res* 1991;51:1452–9.
  25. Dolf G, Meyn RE, Curley D, et al. Extrachromosomal amplification of the epidermal growth factor receptor gene in a human colon carcinoma cell line. *Genes Chromosomes Cancer* 1991;3:48–54.
  26. Moroni M, Veronese S, Benvenuti S, et al. Gene copy number for epidermal growth factor receptor (EGFR) and clinical response to antiEGFR treatment in colorectal cancer: a cohort study. *Lancet Oncol* 2005;6:279–86.
  27. Rafehi H, Orłowski C, Georgiadis GT, et al. Clonogenic assay: adherent cells. *J Vis Exp* 2011;49:e2573. <http://doi.org/10.3791/2573>
  28. Zembruski NC, Stache V, Haefeli WE, et al. 7-Aminoactinomycin D for apoptosis staining in flow cytometry. *Anal Biochem* 2012;429:79–81.
  29. Seger R, Krebs EG. The MAPK signaling cascade. *FASEB J* 1995;9:726–35.
  30. Stephens RM, Yi M, Kessing B, et al. Tumor RAS gene expression levels are influenced by the mutational status of RAS genes and both upstream and downstream RAS pathway genes. *Cancer Inform* 2017;16:1176935117711944.